Experimental study on impact of drying on structural performance of reinforced concrete shear wall

Supported by a Grant-in-Aid for Scientific Research (B) (Grant No. 15H04077)

Hiroshi Sasano[1] and Ippei Maruyama[2*]

[1]Ph.D student, Graduate School of Environmental Studies, Nagoya University, Nagoya, Japan.

[2]Professor, Graduate School of Environmental Studies, Nagoya University, Nagoya, Japan. *Corresponding author, Email: ippei@dali.nuac.nagoya-u.ac.jp

Abstract

The aim of this study is to experimentally investigate the effect of drying on a shear wall, and to clarify the mechanism behind the changes in the structural performance due to drying. Two sufficiently hydrated wall specimens are prepared. Then, one is loaded without drying, while the other is tested after drying for long enough to reach an equilibrium state. The results show a reduction in the initial stiffness and little change in the ultimate shear strength in the dry specimen, in spite of an increase in the compressive strength.

1. Introduction

After demolding, it is inevitable for concrete to be exposed to ambient air to dry, and this drying process will take a long time until an equilibrium state is reached. In general reinforced concrete (RC) structures, concrete shrinkage due to drying is restrained by rebars and adjacent members, which can result in cracks.

In addition, drying affects the concrete in the multi-scale as well as the macro-scale, such as in drying shrinkage-induced cracking. On the nano-scale, changes in the physical characteristics of a calcium-silicate-hydrate (C-S-H) of cement paste have been reported (Maruyama *et al.* 2014a). On the sub-milli-scale, microcracks occur due to the difference in the shrinkage of the aggregate and cement paste (Bisschop and Van Mier 2002; Idiart *et al.* 2012; Maruyama *et al.* 2012). As a result, macroscopic properties, such as the Young's modulus and the compressive/tensile strength, change due to drying (Maruyama *et al.* 2014b). In particular, it has been reported that the Young's modulus of concrete decreases as drying progresses.

Meanwhile, a long-term decrease in the natural frequency has been observed in nuclear power plants and middle to high story RC buildings (Ikawa *et al.* 2012; Maruyama 2016; Morita *et al.* 2016). A theory to explain this phenomenon is the effect of drying on the RC structure (Maruyama 2016). As Maruyama has pointed out, a decrease in the Young's modulus due to drying and drying shrinkage-induced cracks contribute to the stiffness reduction of the structure, which translates to a decline in the natural frequency. It is noteworthy that no stiffness change has been observed during small and medium earthquakes in 8 story steel-reinforced concrete (SRC) buildings (Li *et al.* 2014).

Based on the above, in order to maintain the long term safety of buildings, it is necessary to appropriately evaluate and predict the changes in the structural performance due to drying. The natural frequency reduction may cause unexpected resonance between structures and installments in important structures such as nuclear power plants, as well as unexpected excessive deformation during earthquakes in medium to high story buildings.

Many experimental and numerical studies have been conducted on the influence of drying and the resultant shrinkage on RC structural performance. For example, studies exist on the effect of shrinkage due to self-strain stress without considering concrete alternation (Umemura 1955; Aoyama 1958), the time dependent change in the stiffness of beams and slabs considering shrinkage, creep, and macroscopic cracks (Al-Deen *et al.* 2011; Gilbert 2013), tensile experiments of RC prisms (Bischoff 2001; Ema *et al.* 2002), the bending crack strength and ultimate bending strength of columns and beams (Iso *et al.* 1993; Tanimura *et al.* 2007; Lampropoulos and Dritsos 2011; Gribniak *et al.* 2013), and the shear strength (Sato and Kawakane 2008; Mitani *et al.* 2011; Nakarai *et al.* 2016; Nakarai *et al.* 2017). In tensile experiments of RC prisms, it was observed that drying shrinkage brought about a reduction in the apparent cracking load and made the softening steep (Gilbert 2013). With regard to the bending, a reduction in the bending crack strength has been commonly observed. In the ultimate bending strength, no significant changes have been reported. Iso *et al.* (1993) has reported that the standard formula could evaluate the bending strength of desiccated column specimens. Lampropoulos and Dritsos (2011) numerically confirmed that drying shrinkage decreased the ultimate bending strength of RC columns, and that simulation considering shrinkage reproduced the experimental result more precisely than that without shrinkage. Regarding the influence on the shear behavior, Nakarai *et al.* (2016) observed that the shear crack strength and ultimate strength of beams decreased in both cases with or without shear reinforcement as drying shrinkage increased. In numerical investigations, the changes in the structural performance of RC beams which show shear failure (Gebreyouhannes and Maekawa 2011; Gebreyouhannes *et al.* 2014), and in the dynamic response of an 8 story RC building (Chijiwa and Maekawa 2015) were reproduced, using a multi-scale numerical model '*DuCOM-COM3*' developed by Maekawa *et al.* (2003).

However, although some studies have reported the effect of drying on walls (Yoshida *et al.* 1987; Sashima *et al.* 2008; Hosoya *et al.* 2016; Maruyama 2016; Tadokoro *et al.* 2017), these are not sufficient to establish a common view and little has been done to examine the mechanism of how the drying affects the structural performance of the wall. Sashima *et al.* (2008) conducted loading experiments on walls with drying shrinkage-induced cracks and reported a decrease in the initial stiffness and the same maximum load as non-drying walls. Hosoya *et al.* (2016) and Tadokoro *et al.* (2017) carried out a loading test of shear walls, simulating the cracks due to drying and earthquake using previously repeated-loads. They found that, compared with specimens without initial cracks, the wall with a wall reinforcement ratio of 0.66% decreased in ultimate strength by 5%, while those with a ratio of 1.32% showed no change in strength. This indicates that the effect of drying changes depending on the reinforcement ratio. Maruyama (2016) pointed out that: 1) drying reduced the initial stiffness by about 50% at the equilibrium of moisture transfer, 2) shrinkage-induced cracks contributed more to stiffness reduction than to decreases in the Young's modulus of concrete due to drying, based on 2D non-linear finite-element-method (FEM) coupled with a moisture transfer analysis. Kurihara *et al.* (2017) conducted a parametric study of a shear-wall dominant RC structure on the curing period, and the scale-effect of drying numerically. As a conclusion, they pointed out that the natural frequency changes could be reproduced, and that the specimen scale significantly affected the aging changes of the initial stiffness due to drying, as well as the stiffness after long term drying (50 years).

To sum up, while an initial stiffness reduction has been commonly observed, the method to evaluate changes in the structural performance quantitatively and a common view on the effect of drying on the strength of walls have yet to be established. Furthermore, no mechanism has been discovered to explain those experimental results.

Based on previous research, the present study attempted to understand the effect of pure drying on a RC shear wall using experiments. Two wall specimens were prepared for control and drying, with both being subjected to moist curing for about 100 days in order to avoid an additional progression of the hydration during drying. Subsequently, one was loaded without drying, and the other was loaded after being subjected to drying in ambient air for 1 year to achieve a moisture condition equilibrium.

2. Experimental outline

2.1. Concrete mixture properties and rebar properties

Table 1 and **Table 2** show the physical properties of the cement and aggregate, and the mixture proportions of the concrete. To investigate the effect of drying on the structural performance, the concrete mixture was designed to contain large amounts of water to promote drying shrinkage. The maximum size of the coarse aggregate was 15 mm, considering the workability, because the wall specimens are of a smaller scale than actual buildings.

As shown in **Table 3**, three types of rebar were used depending on their parts. Material properties of each rebar were obtained from direct tensile tests and 3 specimens were prepared for each type of rebar. In the case of D4, a 0.2% offset value was adopted for the yielding strength (f_y) because D4 did not show a clear yielding point.

Table 1 Physical properties of cement and aggregates.

Material	Notation	Properties
Cement	C	Ordinary Portland cement
Water	W	-
Coarse aggregate	G	Seto Mountain gravel G: 60%, ρ_{DRY}: 2.55g/cm^3, ρ_{SAT}: 2.58g/cm^3 Maximum particle size: 15mm
Fine aggregate	S	Seto Mountain sand G:2.8%, ρ_{DRY}: 2.51g/cm^3, ρ_{SAT}: 2.55g/cm^3
Agent	AE	AE water reducing agent

G: Solid volume percentage, ρ_{DRY}: Density at the oven dry condition, ρ_{SAT}: Density at the saturated surface dry condition

Table 2 Mixture proportions and fresh properties of concrete.

Mixture proportion							Fresh Properties		
W/C (%)	s/a (%)	Mass (kg/m^3)					Slump (cm)	Air (%)	Temp. (°C)
		W	C	G	S	AE			
56.3	50	182	324	864	854	3.24	18	5.0	8

Table 3 Material properties of rebar.

	Position	Type of steel	E_s (GPa)	f_y (MPa)	ε_y (10^{-6})	f_u (MPa)
D4	Wall	SD295A	177	367*	2073	523
D6	Column (stirrups)	SD295A	182	347	1907	460
D10	Column (longitudinal reinforcement)	SD345	199	382	1920	550

*0.2% offset value

2.2. RC wall specimen preparation and curing

Table 4 and **Fig. 1** show specifications and a schematic of the RC walls, respectively. The wall specimen was prepared at about a 1/3 scale and was designed to fail in shear. The thickness of the wall was 80 mm and the cross section of the column was 200×200 mm. The wall reinforcement ratio was 0.35% and the longitudinal and transverse reinforcement of the columns were 2.85% and 0.32%, respectively, which meet the RC standard of Japan (Aij 2010). In **Table 4**, calculated strength (i.e., a shear crack load, an ultimate shear strength, and an ultimate bending strength) according to "Design Guidelines for Earthquake Resistant Reinforced Concrete Buildings Based on Inelastic Displacement Concept" (DGEI) (Aij 1999) and Japanese RC standard (Aij 2010) are shown. As shown in **Fig. 4**, the shear span ratio of the wall is 0.32, and the natural axis was kept at the center of the wall height during the loading test.

In this study, two types of wall specimen, named "Sealed" and "Dry", were prepared. Both specimens were cast at the same time, and then 7 days of sealed initial curing and moisture curing until the age of 87 days (Sealed specimen) or 104 days (Dry specimen) was reached. Afterwards, the Sealed specimen was loaded at the age of 94 days (exposed to ambient air for 7 days because of the measurement preparation). In the Dry case, the specimen was subjected to drying (ambient air in the experimental room) for approximately 1 year (until the age of 462 days was reached) and then loaded. As shown in **Fig. 2**, an average temperature and relative humidity during the drying period were 18.4°C and 58.7% R.H., and the maximum and minimum temperatures were 34.3°C and 3.1°C. Little difference between ambient air and in-wall temperature was observed.

Table 4 Specimen specifications.

Wall									
h	l	t	Wall rebar	p_w (%)	Shear span	Shear span ratio: a/d (-)	Calculated value		
							Shear crack load (kN)	Ultimate shear strength (kN)	Ultimate bending strength (kN)
1100	1300	80	2-D4@100 ($26mm^2$)	0.35	550	0.32 (550/1700)	498[1)]	904[2)] 817[1)]	1830[3)]

1) DGEI formula (the mean formula for the effective compressive coefficient $\nu=0.8-\sigma_b/200$ is used, σ_b: compressive strength of the cylinder (N/mm^2)), 2) Arakawa mean formula (*Shear span ratio is outside the scope ($1<a/d<3$)), 3) AIJ standard

Column						
h	b	d	Longitudinal rebar	p_{gc} (%)	Stirrup	p_{wc} (%)
1100	200	200	16-D10 (1136mm^2)	2.85	2-D6@100 (64mm^2)	0.32

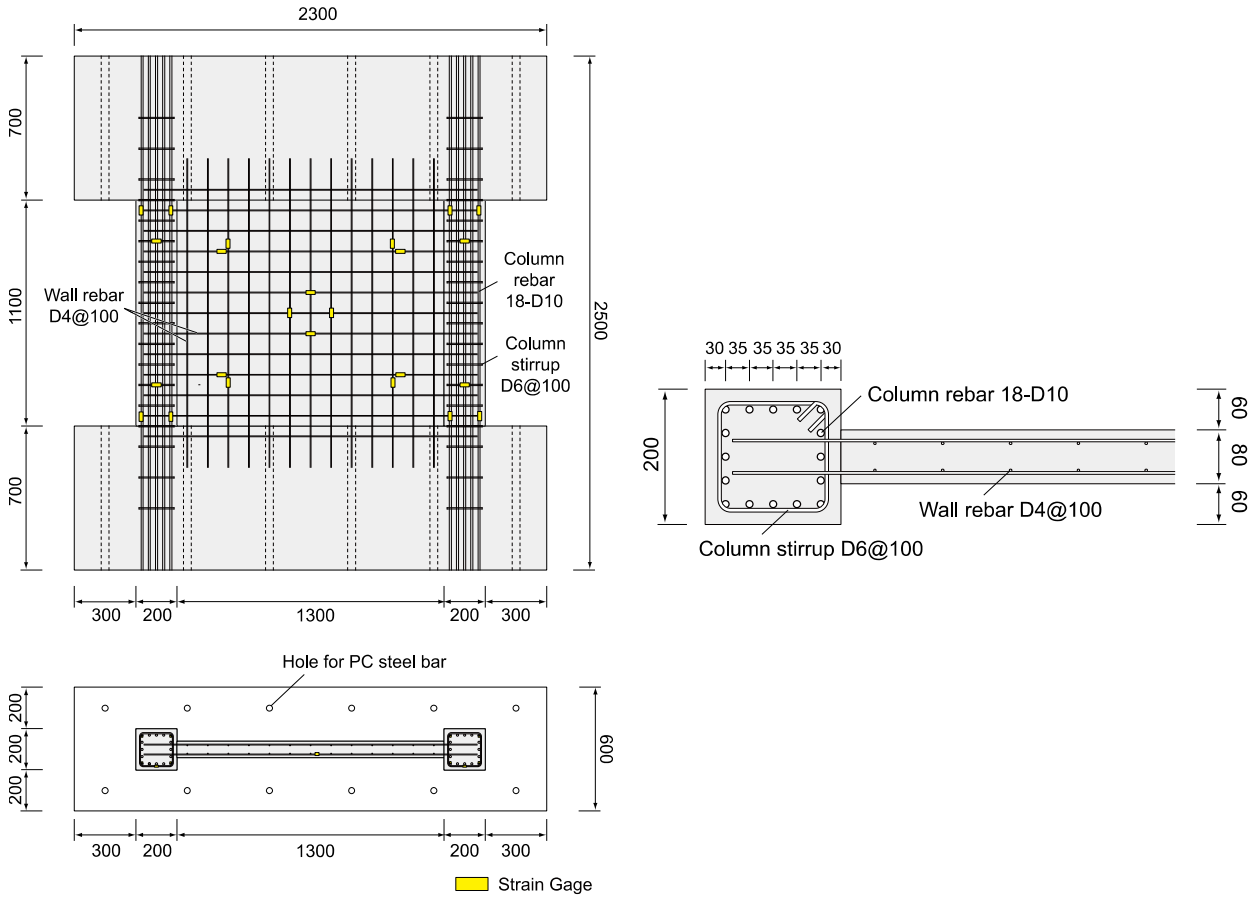

(a) Overall (b) Details of the wall and column

Fig. 1 Schematic of the RC wall specimen.

2.3. Concrete properties

Material property testing and drying shrinkage measurements were conducted. The compressive strength, Young's modulus, and tensile-splitting strength were tested at the age of loading with a cylinder of concrete of φ100×200mm, according to the Japanese Industrial Standard (JIS A 1108, JIS A 1149, and JIS A 1113, respectively). Tensile fracture energy tests were conducted using 100×100×400 mm concrete specimens with a notch of 30 mm in depth, according to JCI-S-001-2003 (Jci 2003).

Drying shrinkage was measured with 2 types of specimen: one 1000×1000×80 mm concrete plate specimen, which imitate a wall specimen (dummy specimen), as shown **Fig. 3**, and two φ100×200 mm cylinder specimens. One dummy specimen and two cylinder specimens were prepared and desiccated in ambient air (same condition as the wall specimen). The four sides of the dummy specimen were sealed using aluminum tape, and the shrinkages were

measured using 2 embedded strain gauges. In the case of cylinder specimens, shrinkage was measured using a height gauge (QM-Height 350, accuracy: (±2.8+5*L*/1000) μm, *L*: measuring length (mm); Mitutoyo, Kawasaki, Japan) without any sealing, and acrylic plates were attached to the head of the specimens for measurements.

The properties of the specimens are shown in **Table 5**. All specimens were cured and tested in the same conditions as each wall.

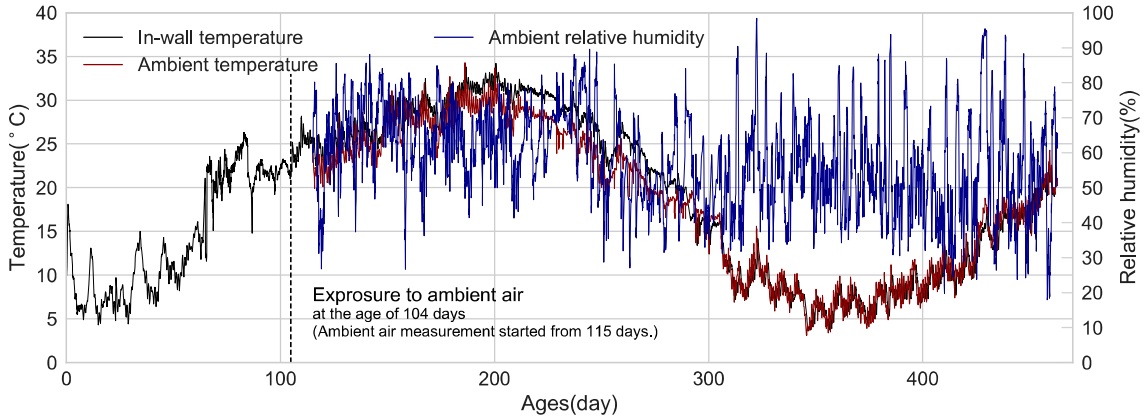

Fig. 2 History of temperature and humidity.

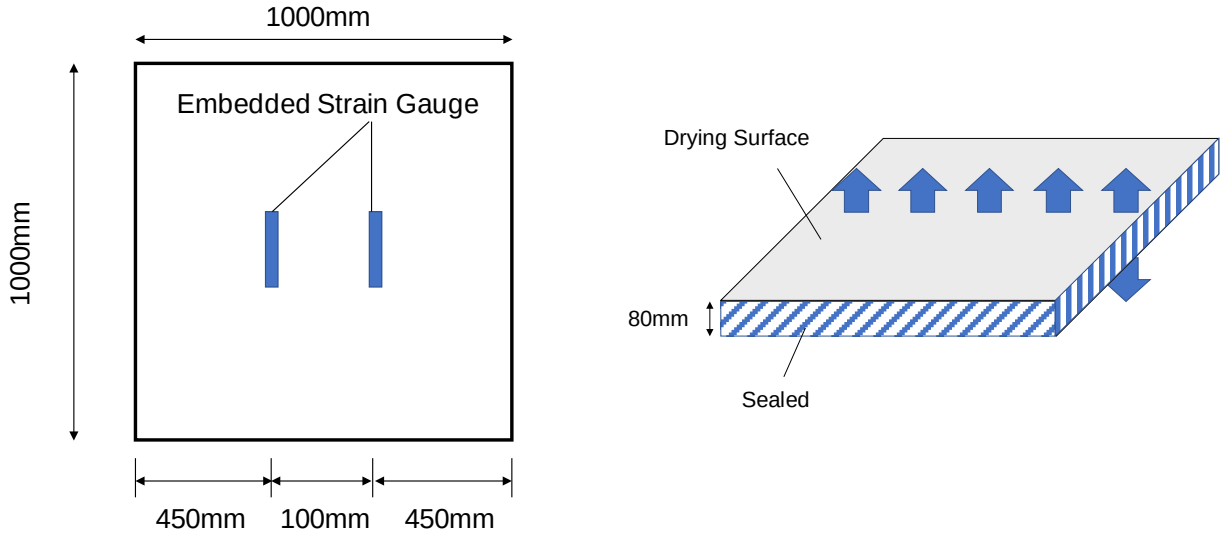

(a) Strain gauge position (b) Drying condition

Fig. 3 Dummy specimen for shrinkage measurement.

2.4. Loading tests of the RC wall specimens

As shown in **Fig. 4**, the wall specimens were loaded so as to generate a reverse symmetric moment, and a pentagram keeps upper and lower stubs parallel during loading; that is, the pentagram restrained both top and bottom stubs for rotation. The shear span ratio was fixed at 0.32. An axial force of 360 kN was applied during loading, which was associated with an axial force ratio of 0.15 in each column for the designed compressive strength of 30 MPa. The axial force was kept constant during loading. The loading process started from a story drift angle of ±1/3200,

and then doubled. From the drift angle of ±1/400, the cycle was repeated twice. In Sealed case, ±1/3200 cycle was repeated twice in order to adjust the wall to the equipment (i.e., ±1/3200→(±1/3200(2): only Sealed)→±1/1600 →±1/800→±1/400→±1/400(2)→±1/200 (Sealed failed at 1/220)→1/170: Dry failed).

The measurement system is shown in **Fig. 1(a)** and **Fig. 5**. Measurement of the rebar strain was conducted from the time of casting, and the drift angle of the wall was calculated based on the horizontal deformation between stubs using contact type displacement meters and a frame attached behind the stub.

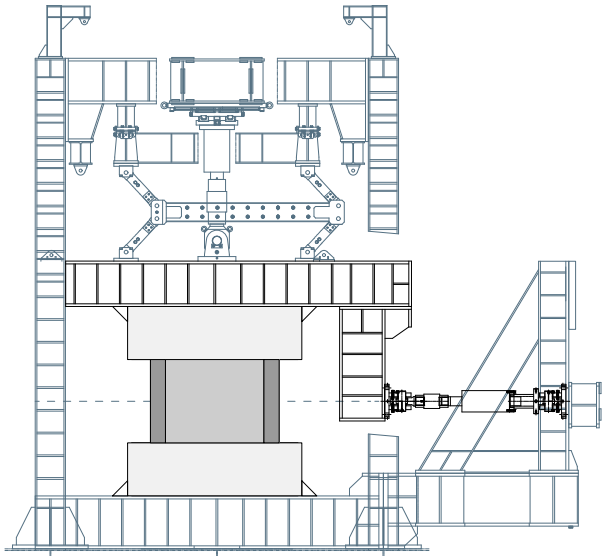

Fig. 4 Loading device.

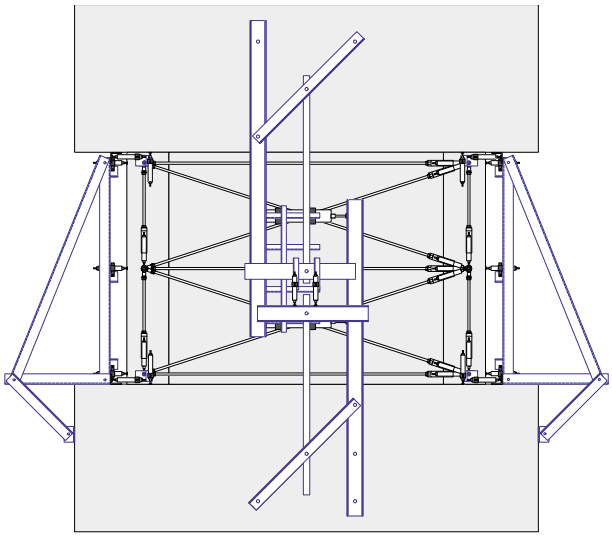

Fig. 5 Measurement system.

3. Experimental results

3.1. Material properties and drying shrinkage of concrete

Table 5 shows the compressive strength (f_c), Young's modulus (E_c), tensile splitting strength (f_t), and tensile fracture energy (G_{ft}) before and after drying with standard deviation (*n* in the table represents the number of specimen). The number in brackets shows the normalized properties (Dry properties/Sealed properties). A 7% increase in compressive strength and a 14% decrease in the Young's modulus for the Sealed condition were observed. Although a mature concrete strength reduction of around 60% at the R.H. equilibrium state was reported (Maruyama *et al.* 2014b), in this study, the increase in strength due to additional hydration during drying seemed to exceed the effect of drying. On the other hand, the Young's modulus reduction can be interpreted as the influence of the microcrack exceeding the additional hydration effect. It may be worth mentioning here that the compressive strength, 36.5±0.5MPa (n=3), was also measured at the age of 28 days under standard water curing, which was almost same as for 87 days (Sealed). For the tensile splitting strength, almost no change was observed between the Sealed and Dry specimens. The tensile fracture energy of the Dry specimens was 46% higher than for the Sealed. This may have been caused by microcracks and C-S-H alternation, and similar trend has been reported (Matsuzawa and Kitsutaka 2013).

The shrinkage of the wall dummy and cylinder specimens during the drying period is shown in **Fig. 6**. From **Fig. 6(a)**, it is clear that the drying shrinkage of the dummy specimen had reached the equilibrium state, which implies that the wall specimen also reached equilibrium because it was of the same thickness. The average ultimate shrinkage

was -903 μ in the dummy specimen, and a similar result was found for the average -965 μ shrinkage in the cylinder specimen.

Table 5 Measured material properties of concrete at the age of the RC loading test.

	Age	f_c (MPa)	E_c (GPa)	n	F_t (MPa)	n	G_{ft} (N/m)	n	Cal.*
Sealed	87	35.5±0.24	30.4±0.27	3	3.1±0.29	4	87.9±4.4	4	81.1
Dry	462	39.0±0.44 (1.10)	26.0±0.88 (0.86)	5	3.0±0.57 (0.97)	5	128.7±11.7 (1.46)	4	-

*Calculated according to JSEC standard (Jsce 2002)

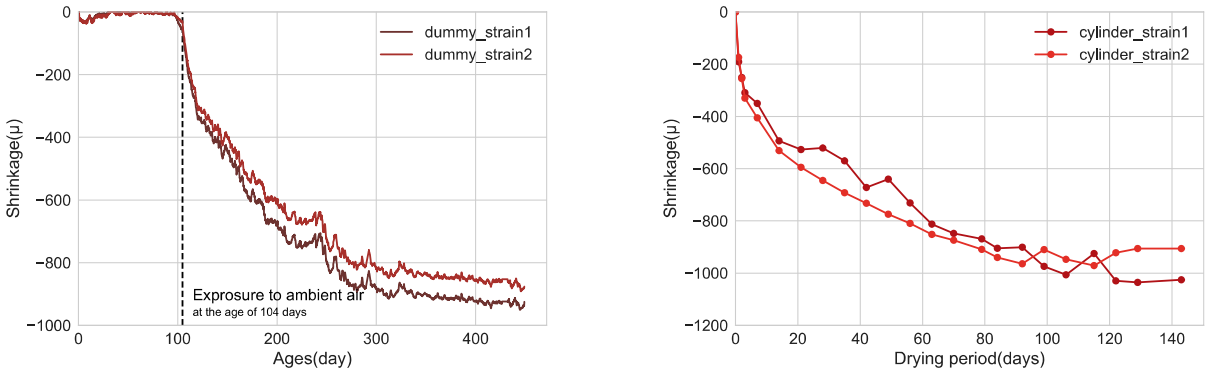

(a) Dummy: average -901 μ

(b) Cylinder: average -965 μ

Fig. 6 Drying shrinkage of concrete.

3.2. Shrinkage induced cracks of the wall

Figure 7 shows the drying shrinkage-induced crack pattern, which was observed just before loading. The values in **Fig. 7** indicate the crack width (unit: mm); cracks without value indicate the width of the entire crack was less than 0.03 mm. The maximum crack width was 0.15 mm, which locations were the upper left (front side) and lower left corner (back side) of the wall restrained by the stub and column. Crack widths were measured at 86 points in total (average interval was about 10 cm), and the average crack width was about 0.05 mm.

Figure 8 shows the rebar strain after drying (slashed area means there was no data because of disconnection). Almost all the measurement points (25 out of 28) showed shrinkage strain, and the maximum shrinkage was -827 μ in the horizontal direction at the center of the wall. The wall reinforcement at the lower and upper left corner showed tensile strain; these regions corresponded to the location of drying shrinkage-induced cracks shown in **Fig. 7**. The maximum tensile strain was 323 μ in the vertical direction at the lower left corner of the wall.

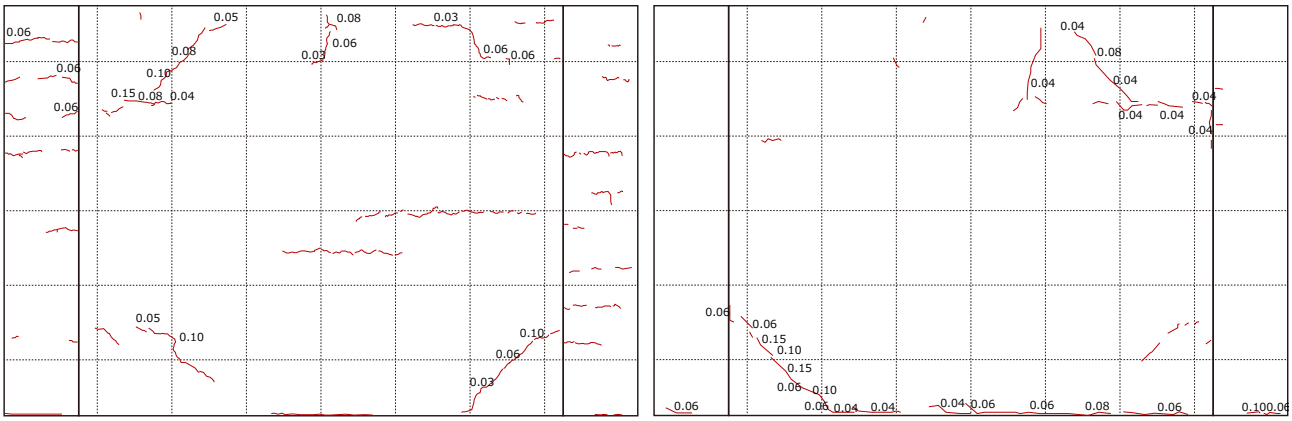

(a) Front (right side is north) (b) Back (right side is south)

Fig. 7 Drying shrinkage-induced crack at the end of drying (at the age of 462 days).

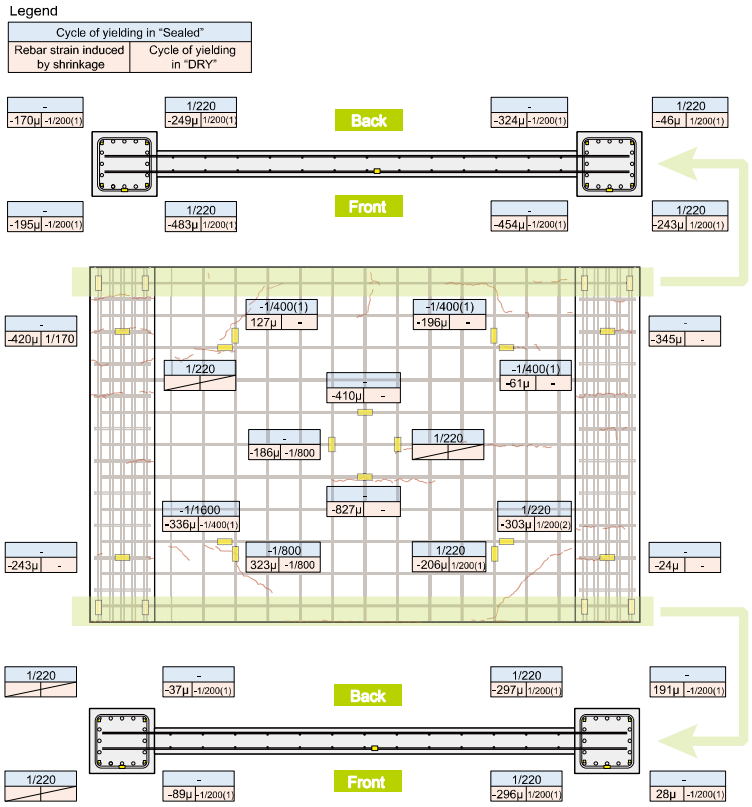

Fig. 8 Rebar strain of the wall after drying and the load rebar yielding.

3.3. Loading test results

3.3.1. Overall results

Figure 9 and **Fig. 10** show the load-deformation relationship obtained by the loading test with the theoretical stiffness (shape factor (κ) for shear stiffness was calculated following the AIJ standard (Aij 2016)). Since both walls showed brittle failure, few data points in the post-peak were measured. **Table 6** shows a list of load and displacement at significant stages. Compared with the Sealed specimen, a reduction was seen in the initial stiffness, the shear crack load (decreased by 160 kN), and the yielding load of the column reinforcement (decreased by 85 kN). The ultimate strength was slightly lower (decreased by 40 kN, Dry/Sealed: 0.96) and the deformation due to the strength increased by 1.1 times more than the Sealed specimen. The deformation at the shear cracking load and the rebar yielding load of the column was almost the same between the Sealed and Dry specimens. It should be noted that despite a 10% increase in the compressive strength after drying (see Table 5) the ultimate strength of the Dry wall was almost the same. This phenomenon cannot be explained by existing standard formulas of the ultimate shear strength (*e.g.*, Arakawa formula (Aij 2010), the DGEI formula (Aij 1999). This point is argued in Section 5 using numerical results.

Table 7 indicates the stiffness of each cycle. The initial stiffness was calculated using a linear least-squares method using data from the origin to the positive peak in the 1/3200 cycle. The equivalent stiffness of each cycle was the average of the two slopes connecting the origin and the positive/negative peak. In this table, it is clearly observed that the initial stiffness after drying decreased by half; as deformation increased, the difference in the equivalent stiffness became smaller.

The crack pattern after failure is illustrated in **Fig. 11**; the gray parts indicate spalling at failure. Both the Sealed and Dry specimens showed brittle failure, and no change in the failure mode was observed. Clearly, more cracks were observed in the Dry wall, as **Fig. 11** shows. This can be explained as the initial stress and shrinkage-induced cracks promoting the generation of new cracks at the time of loading. In the Dry specimen, the progress of cracks induced by drying shrinkage (initial cracks) were observed during the first cycle (1/3200), and it seemed to contribute to the initial stiffness reduction and the occurrence of shear cracks. Focusing on the cracks at failure, it was observed that new cracks had occurred connecting to the existing cracks, which led to failure; that is, cracks at failure appeared independently of the shrinkage-induced cracks.

In short, drying and cracks induced by shrinkage had significant influence on the initial stiffness and the shear crack strength of the wall. On the contrary, little changes or slight decreases in the ultimate strength were observed despite the 10% increase in compressive strength. This is discussed fully in **Chapter 5**.

3.3.2. Comparison of the initial stiffness

The initial stiffness reduction of 0.54 times is compatible with the natural frequency reduction of 0.73 times following equation by assuming the elastic response and the same vibration mode:

$$\boldsymbol{f/f_0 = \sqrt{E/E_0}} \quad (1)$$

where f: natural frequency after drying(Hz), f_0: initial natural frequency (Hz), E: initial stiffness(kN/mm), and E_0: initial stiffness before drying (kN/mm). In this equation, weight of a building is assumed to change little by aging.

The value of 0.73 times in natural frequency is quite close to the values shown in the previous reports concerning the natural frequency change of the existing buildings (*i.e.*, the SRC building, and the nuclear power plants) which

age are more than 10 years (Maruyama 2016; Morita *et al.* 2016). It was concluded that the impact of drying on the stiffness of RC wall and resultant natural frequency change was experimentally confirmed in this study.

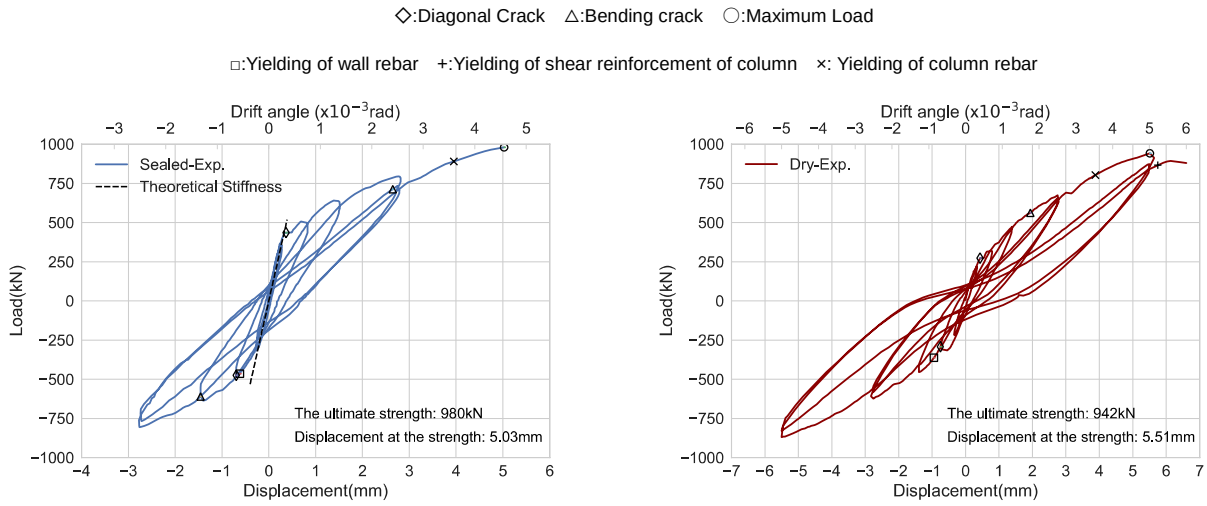

(a) Sealed (b) Dry

Fig. 9 Load-deformation relationships.

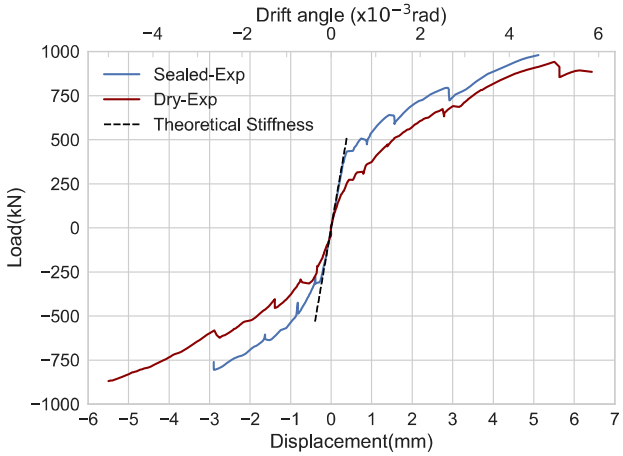

Fig. 10 Envelopes of each specimen.

Table 6 Load and displacement at significant stages of loading.

	Shear crack		Yielding of wall rebar		Bending crack		Yielding of column rebar		Ultimate strength	
	Load	Disp.	Load	Disp.	Load	Disp.	Load	Disp.	Load	Disp.
Sealed	435	0.37 (1/2970)	-464	-0.62 (1/1770)	-610	-1.46 (1/753)	889	3.95 (1/278)	980	5.02 (1/220)
Dry	273	0.435 (1/2530)	-362	-0.95 (1/1160)	562	1.94 (1/567)	804	3.88 (1/284)	942	5.51 (1/200)

*Values in brackets shows drift angle. (Unit of “Load”: kN, Unit of “Disp.”: mm)

Table 7 Stiffness of each cycle.

		Sealed	Dry	Theoretical stiffness*2	Dry /Sealed	Dry /Theoretical
Initial Stiffness (kN/mm)		1226	663	1330	0.54	0.50
Equivalent Stiffness (kN/mm)	1/800	459	333	-	0.73	0.25
	1/400	289	236		0.82	0.18
	1/200	196*1	165		0.84	0.12

*1: Calculated by the least squares method of the load deformation relation from 0 kN to the failure (1/220)

*2: Shape factor is calculated by the "AIJ standard for Lateral Load-carrying Capacity Calculation of Reinforced Concrete Structures (Draft)" (Aij 2016)

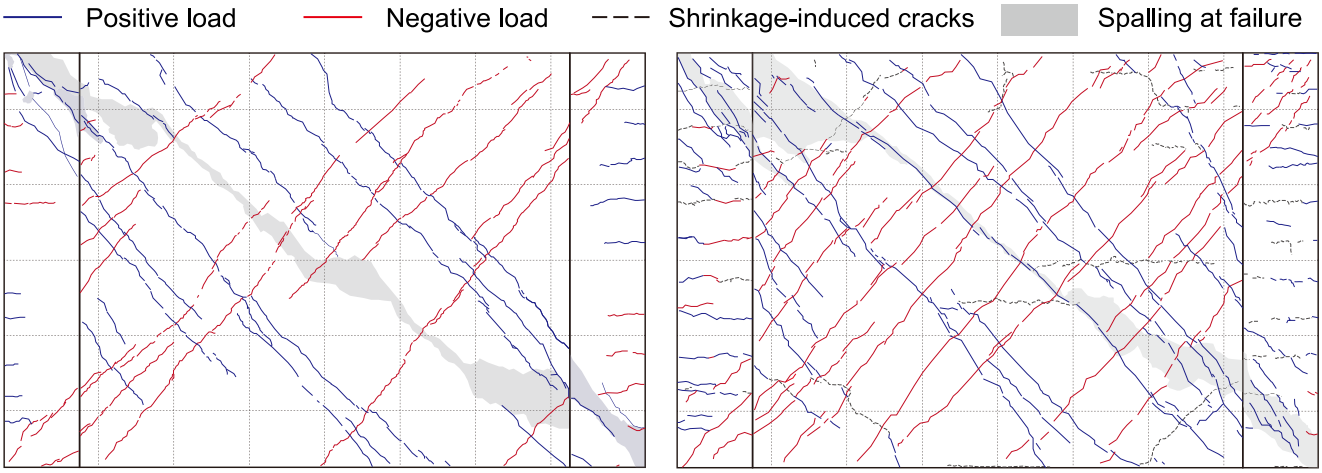

(a) Sealed: failure at 5.03 mm (1/220) (b) Dry: failure at 6.44 mm (1/170)

Fig. 11 Crack pattern at failure.

4. Conclusion

In the present study, so as to reveal the influence of drying and the resultant cracks on the structural performance of RC shear walls, an experiment and analysis were conducted.

A loading experiment on a matured RC wall, which had been kept sealed until loading, and on a wall which was subjected to drying, after moisture curing during almost the same period as the sealed specimen, was carried out. In this experiment, the influence of hydration was eliminated to the upmost (*i.e.*, the moisture curing period was more than 87 days) and the drying period was sufficient for the moisture content of the wall to reach the equilibrium state. The results were as follows:

1) With regard to concrete properties after drying, the compressive strength was 10% higher, the Young's modulus was 14% lower, the tensile splitting strength was almost same, and the tensile fracture energy was 46% higher than the sealed one.
2) The initial stiffness of the wall after drying decreased 46% compared with the sealed specimen, and the initial stiffness of the sealed specimen corresponded with the theoretical stiffness.
3) Both the sealed and dry walls showed shear failure and the same failure mechanism. The ultimate strength was almost same: 980 kN for the Sealed and 942 kN for the Dry. Furthermore, the horizontal displacement at the ultimate strength was increased after drying: 1/171 rad in the Sealed and 1/200 rad in the Dry.

Acknowledgements

This work was supported by a Grant-in-Aid for Scientific Research (B) (Grant No. 15H04077).

References

Aij (1999). "*Design guidelines for earthquake resistant reinforced concrete buildings based on inelastic displacement concept.*" Tokyo: Architectual Institute of Japan.

Aij (2010). "*Aij standard for structural calclation of reinforced concrete structures revised 2010.*" Tokyo: Architectural Institute of Japan.

Aij (2016). "*Aij standard for lateral load-carrying cpacity calculation of reinforced concrete structures (draft).*" Tokyo: Architectural Institute of Japan.

Al-Deen, S., Ranzi, G. and Vrcelj, Z. (2011). "Shrinkage effects on the flexural stiffness of composite beams with solid concrete slabs: An experimental study." *Engineering Structures*, 33(4), 1302-1315.

Aoyama, H. (1958). "Influence of inital deformation on the plastic behavior of reinforced concrete frame(structure)." *Transactions of the Architectural Institute of Japan*, 60(1), 617-620 (in Japanease).

Bischoff, P. H. (2001). "Effects of shrinkage on tension stiffening and cracking in reinforced concrete." *Canadian Journal of Civil Engineering*, 28(3), 363-374.

Bisschop, J. and Van Mier, J. G. M. (2002). "How to study drying shrinkage microcracking in cement-based materials using optical and scanning electron microscopy?" *Cement and Concrete Research*, 32(2), 279-287.

Chijiwa, N. and Maekawa, K. (2015). "Thermo-hygral case-study on full scale rc building under corrosive environment and seismic actions." *Journal of Advanced Concrete Technology*, 13(10), 465-478.

Ema, T., Ishida, T. and Maekawa, K. (2002). "Effect of dyring shrinkage on rc property under tensile stress." *Proceedings*

of the Japan Concrete Institute, 24(1), 435-440 (in Japanese).

Gebreyouhannes, E. and Maekawa, K. (2011). "Numerical simulation on shear capacity and post-peak ductility of reinforced high-strength concrete coupled with autogenous shrinkage." *Journal of Advanced Concrete Technology*, 9(1), 73-88.

Gebreyouhannes, E., Yoneda, T., Ishida, T. and Maekawa, K. (2014). "Multi-scale based simulation of shear critical reinforced concrete beams subjected to drying." *Journal of Advanced Concrete Technology*, 12(10), 363-377.

Gilbert, R. I. (2013). "Time-dependent stiffness of cracked reinforced and composite concrete slabs." *Procedia Engineering*, 57, 19-34.

Gribniak, V., Kaklauskas, G., Kliukas, R. and Jakubovskis, R. (2013). "Shrinkage effect on short-term deformation behavior of reinforced concrete – when it should not be neglected." *Materials and Design*, 51, 1060-1070.

Hosoya, N., Koike, T., Suzuki, Y., Maeda, T., Tsurukai, K. and Ogata, Y. (2016). "Study on damage and deterioration of structural performance in rc shear walls part 1 outline of experimental plan and results of the specimen without damage." *Summaries of technical papers of AIJ annual meeting*, 157-158 (in Japanese).

Idiart, A., Bisschop, J., Caballero, A. and Lura, P. (2012). "A numerical and experimental study of aggregate-induced shrinkage cracking in cementitious composites." *Cement and Concrete Research*, 42(2), 272-281.

Ikawa, N., Fujii, A., Ito, S. and Furuki, T. (2012). "Evaluation of earthquake response of high-rise building during the 2011 off the pacific coast of tohoku earthquake." *Konoike Construction Co. Ltd. Technical Report*, 53-58 (in Japanese).

Iso, M., Yamamoto, T. and Ohtaki, T. (1993). "Experimental study on bending-shear behavior of reinforced concrete columns after subjected to seismic load." *Proceedings of the Japan Concrete Institute*, 15(2), 525-530 (in Japanese).

Jci (2003). "*Method of test for fracture energy of concrete by use of notched beam.*" Tokyo: Japan Concrete Institute.

Jsce (2002). "*Standard specifications for concrete structures -2002, inspection.*" Tokyo: Japan Society of Civil Engineers.

Kurihara, R., Chijiwa, N. and Maekawa, K. (2017). "Thermo-hygral analysis on long-term natural frequency of rc buildings with different dimensions." *Journal of Advanced Concrete Technology*, 15(8), 381-396.

Lampropoulos, A. P. and Dritsos, S. E. (2011). "Concrete shrinkage effect on the behavior of rc columns under monotonic and cyclic loading." *Construction and Building Materials*, 25(4), 1596-1602.

Li, L., Nakamura, A., Kashima, T. and Teshigawara, M. (2014). "Earthquake damage evaluation of an 8-story steel-reinforced concrete building using sa-sd curves." *Journal of Structural and Construction Engineering (Transactions of AIJ)*, 79(702), 1107-1115.

Maekawa, K., Ishida, T. and Kishi, T. (2003). "Multi-scale modeling of concrete performance -integrated material and structural mechanics-." *Journal of Advanced Concrete Technology*, 1(2), 91-126.

Maruyama, I. (2016). "Multi-scale review for possible mechanisms of natural frequency change of reinforced concrete structures under an ordinary drying condition." *Journal of Advanced Concrete Technology*, 14(11), 691-705.

Maruyama, I., Nishioka, Y., Igarashi, G. and Matsui, K. (2014a). "Microstructural and bulk property changes in hardened cement paste during the first drying process." *Cement and Concrete Research*, 58, 20-34.

Maruyama, I., Sasano, H., Nishioka, Y. and Igarashi, G. (2014b). "Strength and young's modulus change in concrete due to long-term drying and heating up to 90°c." *Cement and Concrete Research*, 66, 48-63.

Maruyama, I., Suzuki, M. and Sato, R. (2012). "Stress distribution and crack formation in full-scaled ultra-high strength

concrete columns." *Materials and Structures*, 45(12), 1829-1847.

Matsuzawa, K. and Kitsutaka, Y. (2013). "Influence of age and cure on fracture properties of concrete subjected to high temperature heating." *Journal of Structural and Construction Engineering (Transactions of AIJ)*, 78(688), 1027-1034.

Mitani, T., Hyodo, H., Ota, K. and Sato, R. (2011). "Discovery and the evaluation of shear strength decrease of reinforced normal-strength concrete beams." *Proceedings of the Japan Concrete Institute*, 33(2), 721-725 (in Japanese).

Morita, K., Kashima, T. and Hamamoto, T. (2016). "Long-term condition monitoring of a src building before and after the 2011 off the pacific coast of tohoku earthquake." *Journal of Structural and Construction Engineering (Transactions of AIJ)*, 81(730), 2037-2044.

Nakarai, K., Morito, S., Ehara, M. and Matsushita, S. (2016). "Shear strength of reinforced concrete beams: Concrete volumetric change effects." *Journal of Advanced Concrete Technology*, 14(5), 229-244.

Nakarai, K., Ogawa, Y., Kawai, K. and Sato, R. (2017). "Shear strength of reinforced limestone aggregate concrete beams." *ACI Structural Journal*, 114(4).

Sashima, Y., Fukuhara, Y., Teraoka, M. and Tanioka, Y. (2008). "Investigation of damage conditions in reinforced concrete shear walls and influence of the damage conditions on earthquake resistant performance of the reinforced concrete shear walls." *Proceedings of annual research meeting Chugoku Chapter, Architectural Institute of Japan (AIJ)*, 31, (in Japanese).

Sato, R. and Kawakane, H. (2008). "A new concept for the early age shrinkage effect on diagonal cracking strength of reinforced hsc beams." *Journal of Advanced Concrete Technology*, 6(1), 45-67.

Tadokoro, M., Hanzawa, M., Hosoya, N., Maeda, M., Jin, K. and Ogata, Y. (2017). "Study on damage and deterioration of structural performance in RC shear walls part 4 static loading test plan for earthquake resistant walls with relatively small reinforcement ratio." *Summaries of technical papers of AIJ annual meeting*, 469-470 (in Japanese).

Tanimura, M., Sato, R. and Hiramatsu, Y. (2007). "Serviceability performance evaluation of rc flexural members improved by using low-shrinkage high-strength concrete." *Journal of Advanced Concrete Technology*, 5(2), 149-160.

Umemura, S. (1955). "Self-distortion stress and ultimate strength of plastic rahmen." *Proceedings of annual research meeting Kanto Chapter, Architectural Institute of Japan (AIJ)*, 31(1), 165-166.

Yoshida, I., Kanemitsu, H., Yamashita, M. and Higuchi, K. (1987). "Seismic analysis of r.C. Pier with earthquake resistant wall." *Proceedings of JSCE*, 1987(386), 349-358 (in Japanese).